SLOPE SCALE MODELING OF SNOW SURFACE TEMPERATURE IN TOPOGRAPHICALLY COMPLEX TERRAIN

J.M. Staples, E.E. Adams, A.E. Slaughter, and L.R. McKittrick
Department of Civil Engineering
Montana State University, Bozeman, MT 59717

ABSTRACT: In mountainous terrain, landscape strongly influences the thermal state of snow. An energy balance model, Radtherm/RT, can be used to account for topography in the calculation of snow temperature. For a specific location, a terrain model can be defined and using a connected ensemble of elements or facets. Each element has a specified terrain type with assigned thermal properties. Meteorological data are applied, and a one dimensional energy balance is calculated for each element. This energy balance includes conduction, convection, radiation, and latent heat; however, the calculation of radiation is unique. Taking into account topography, global position, and time, the model can be used to calculate incoming solar radiation for each facet as well as reflected short wave radiation and the exchange of long wave radiation between terrain surfaces.

Light detection and ranging (LIDAR) topographic data with a one meter resolution were used to create two separate models (on the order of 10^4 m^2) for two test areas at the Yellowstone Club in southwest Montana. Meteorological data were collected for these two slopes and used as input for Radtherm/RT to calculate surface temperature and mass flux for each facet in the model. The results for facets in different locations were compared to investigate the effects of local topography. These results were also compared with measured temperatures and observations of surface hoar growth. Readily available USGS topographic data with a 30 meter resolution were used to create a model (on the order of 10^6 m^2) containing both slopes. For this larger scale model, surface temperatures and mass flux were again calculated and compared with results for the slope scale models. Because LIDAR data are costly to obtain and create very large files, the use of USGS data is preferred for the application of Radtherm/RT in other large areas. At this point, the significant result has been the ability of Radtherm/RT to model surface temperature that varies with local topography at the slope scale.

KEYWORDS: snow surface, temperature, topography, energy balance, modeling, radiation

1. INTRODUCTION

Being thermodynamically unstable, snow exists in a perpetual state of metamorphism. This metamorphism alters the morphologic snow structure which in turn determines many of the thermo-mechanical and optical properties which include strength, density, thermal conductivity, heat capacity, and albedo. Such properties can greatly affect the interaction between the snow surface and the atmosphere. The nature of this interaction can be described and driven by the energy balance at the snow surface. Because the energy transfer at the snow-ground interface is generally weak compared to the energy transfer at the snow-atmosphere interface (Etchevers et al., 2004) and the fact that the temperature at the snow-ground interface remains at or near 0°C, the energy balance and resulting temperature at the snow surface can have a profound effect on snow metamorphism. Understanding and modeling the energy balance in complex topography and the associated surface processes have important implications in water resource management, glacier dynamics, hydrology, climate, and avalanche forecasting (Etchervers et al., 2004; Hock, 2005; Fernádez, 1998).

1.1 *Topography*

In mountainous regions, topography can change drastically in very short distances, and the resulting topographic complexity can lead to wide variations in the energy balance of a snow cover (Fierz et al., 2003). Modeling this energy balance and understanding the partitioning of the energy fluxes between different areas are key components to a wide array of snow models that have been developed for different applications over the last thirty years (Etchevers et al., 2004). However, it has been difficult to conduct the large number of calculations needed to determine the spatial variation of the energy balance (Fierz et al., 2003). An easily measurable result of this variation is snow temperature, which has been known to vary widely with topography (McClung and Schaerer, 1993).

1.2 *Radtherm/RT*

The model used in this project, Radtherm/RT, is a first principles energy balance model commercially available from ThermoAnalytics, Inc. It has its origins in software originally written for the U.S. Army and Air Force to identify the thermal/infrared signatures of vehicles (Johnson, 1991; Johnson 1995; PRISM:3.0, 1991). Adams and McDowell (1991) extended the use of this software to topographically complex terrain. Montana State University and ThermoAnalytics, Inc. collaborated to produce a modified version, called Radtherm/RT, specifically for highway applications in topographically complex terrain (Adams, 1999). Radtherm/RT was tested to calculate pavement temperatures (Adams et al., 2004a) and provided reasonable results (McKittrick et al., 2004). Promising results were also obtained when Radtherm/RT was applied to a section of the Bridger Mountain Range following the formation of a surface hoar layer. This model produced values for temperature and mass flux that seemed to agree with observed conditions (Adams et al., 2004b).

2. METHODS

2.1 *Study Site*

In this study, Radtherm/RT was used to model two small slopes for verification and model evaluation. The two study slopes are located at the Yellowstone Club in the Madison Range of southwest Montana and were the location of previous work by Cooperstein et al. (2004). They are both below timberline in generally wind protected areas which are north facing and south facing at elevations of 2532m and 2757m respectively and at a latitude of about 45 degrees. Both slope angles are about 30 degrees. Each site contained a meteorological station which measured wind speed and direction, air temperature, relative humidity, snow depth, snow surface temperature, snow subsurface temperatures in the top 30cm of snow, incoming short wave radiation, reflected short wave radiation, and incoming long wave radiation. Additional temperature data were recorded for rock outcrops and vegetation with stand-alone thermistor/datalogger units (Onset Corp., -HOBO dataloggers). Manual temperature measurements were taken during weekly visits with dial stem thermometers and a handheld IR thermometer, and for the purposes of model verification, observations of surface hoar were recorded. Because Radtherm/RT calculates mass flux, deposition on to the surface is identified by a positive mass flux when it is assumed that condensation occurs in such a form.

2.2 *Model Application*

The first step in applying this software is creating a terrain model for a specific locale. Highly accurate LIDAR (Light Detection and Ranging) data were used to describe the two sites with a 3D resolution of one meter. Once the topography was loaded, the model geometry could be displayed, represented by a connected assemblage of elements or facets (Figure 1 and Figure 2).

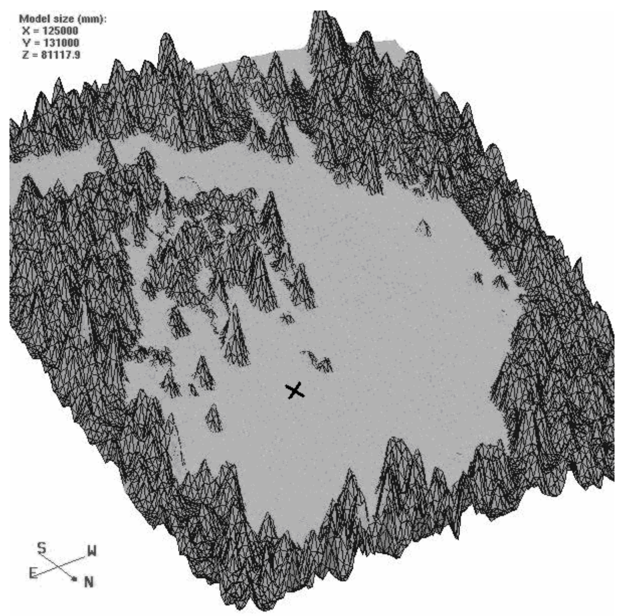

Figure 1: Terrain model of the north facing site built with LIDAR topographic data with an X marking the location of the meteorological station. Because the elements for the snow surface are not distinguishable in this grayscale image, this slope appears to be a flat surface though it actually has variation in its topography.

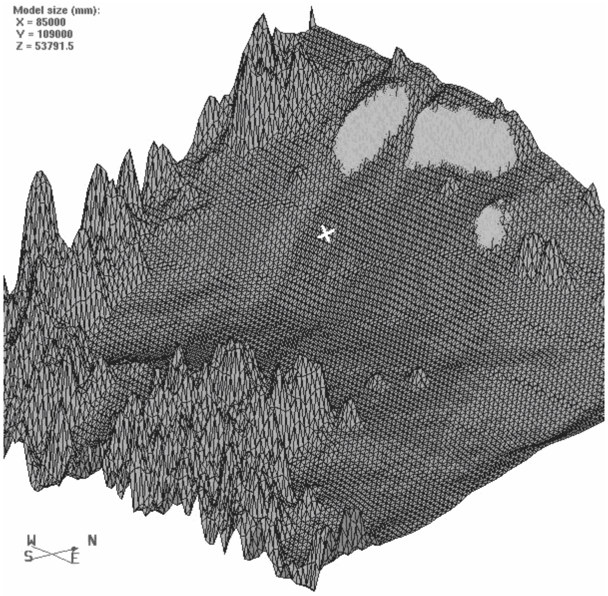

Figure 2: Terrain model of the south facing site built with LIDAR topographic data with an X marking the location of the meteorological station. The lightly shaded regions near the top of the slope are portions of a rock outcrop where surface temperatures were modeled as well as continuously measured and recorded.

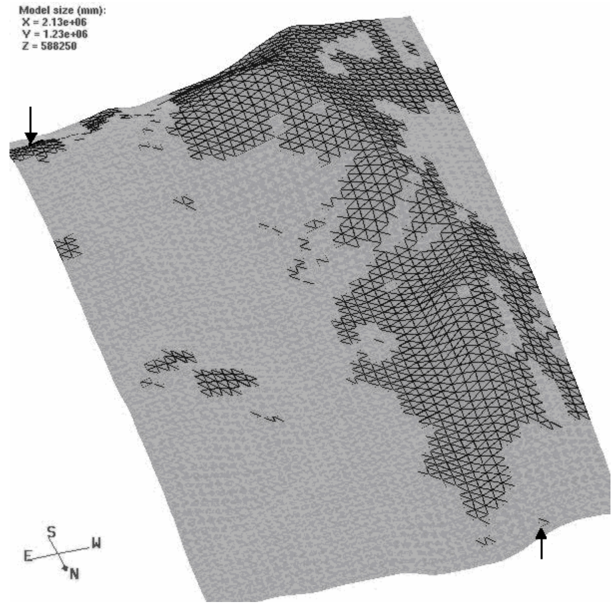

Figure 3: Terrain model built with USGS topographic data. Open, snow covered areas have visible elements in this image, and tree covered areas do not have visible elements as a result of the black and white image. Arrows indicate the approximate locations of the study sites.

The elements are flat surface plates overlying subsurface nodes. Each element is then specified as an appropriate terrain type. In this case, terrain types include coniferous trees, rock, and snow. Each terrain type is assigned specific thermal properties. At this stage of this project, snow thermal properties were based on a rough categorization of snow type. Separate terrain models were built for each site.

In addition to LIDAR data, readily available data from the United States Geological Survey (USGS) were used to define the topography in a model containing both sites (Figure 3). Because such data have a much courser resolution of 30 meters, terrain features can not be identified with as much detail as with LIDAR data. To assign terrain types to each element, land cover data were used in conjunction with the topographic data. Land cover data is readily available from different government agencies, where numbers are assigned to different classes of land cover such as grass, shrubs, deciduous trees, rocks, etc. for each node in the USGS topographic data. These numbers must be then converted to values recognized by Radtherm/RT. Areas identified as grass, scree, and shrub covered were assumed to be snow covered, while tree covered areas and rock outcrops were assumed to be snow free.

Meteorological data collected at the two study sites were used to build a weather file needed to run the software. Required input data include time, air temperature, relative humidity, wind speed, wind direction, incoming short wave radiation, and incoming long wave radiation. Cloud cover and precipitation rate can also be included; however, cloud cover is not needed when incoming long wave radiation is measured, and precipitation rate was not used. With such input data, Radtherm/RT was used to calculate conduction, convection, radiation, and latent heat for each element of the terrain model. Within the snow cover, Fourier's law is solved for each element to calculate the conduction heat flux. A constant snow ground interface of 0°C forms the lower boundary condition, and the upper boundary condition is the flux of the surface energy exchange (Adams et al., 2004b). This flux can be represented by Q:

$$Q = Q_{lw} + Q_{sw} + Q_{lh} + Q_{sh} \qquad (1)$$

The long wave radiation component is Q_{lw}, the short wave radiation component is Q_{sw}, the latent heat component is Q_{lh}, and the sensible heat component is Q_{sh}. Mass flux is determined using the latent heat calculation. The unique strength of Radtherm is the ability to represent the radiation interaction between terrain elements, for both long wave and short wave radiation. Incoming solar radiation is calculated at each time step, while accounting for: topography, global position, and time. The radiation component of Radtherm/RT also includes the calculations of reflected short wave radiation and the long wave radiation exchange between elements. As a result of these calculations for radiation exchange, solar data only needed to be collected at a single “unshaded” point. For instance, solar data for the north site can be collected from the south site, as the instruments collecting data at the north site were subjected to shading. Radtherm/RT then accounts for such shading.

To calculate the radiation exchange, a view factor file must be built following input of topography and land cover. View factors are used to mathematically describe how much sky, vegetation, rock, and snow is visible from each element. For example, an element positioned on a high, bare ridge would “see” mostly sky and very little other terrain. Its resulting temperature might be vastly different from an element positioned in the shade of a tall tree. It is important to understand that view factors are geometrical relationships between all the elements of the specified terrain. Once Radtherm is running, the apparent area for direct solar radiation of each element must be repeatedly calculated to account for movement of the sun throughout the day. View factors, however, are only calculated once as the geometrical relationships between elements do not change.

3. **RESULTS**

The primary focus at this point is to demonstrate the capability of Radtherm/RT to model thermal conditions across the snow surface, including the effects of local topography. Highly accurate LIDAR data has made this possible, where such detailed results are not possible with a more course grid. Surface temperatures and surface mass fluxes were calculated for each element in the model. Differences in temperature between selected elements of snow in the sun and shade and elements of rock and trees were compared to show the effects of local topographic differences and influences of material thermal properties (Figure 4).

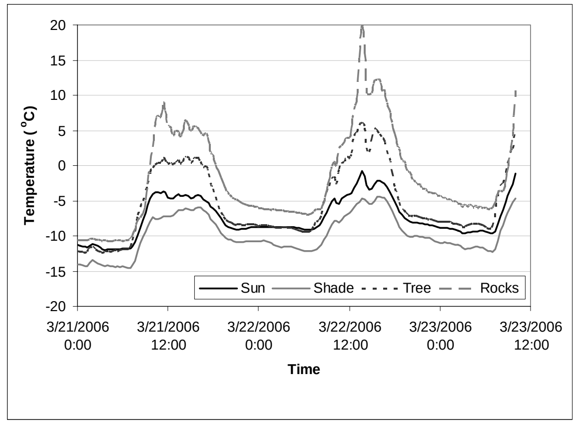

Figure 4: Modeled surface temperatures for elements of snow fully exposed sun, snow fully shaded by trees, the north side of a tree, and a rock outcrop on the south facing site during March 21 to 23, 2006.

As one would expect, snow surface temperatures in the shade were cooler than those exposed to direct sun. Additionally, surface temperatures of a south facing rock element reach much higher values than the nearby snow surface during midday. The temperature of a snow surface element subjected to morning sun and afternoon shade was also compared to snow elements in full sun and full shade (Figure 5).

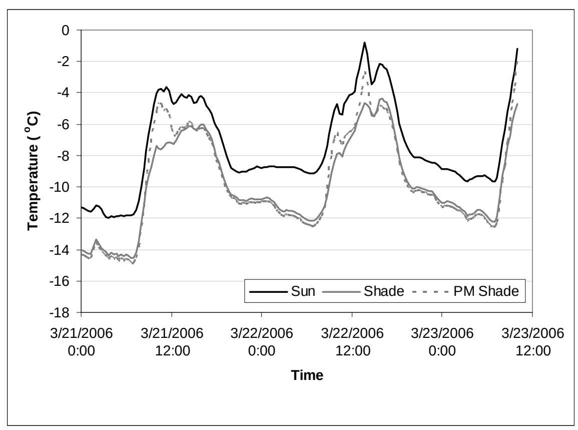

Figure 5: The modeled temperatures of the same sun and shade elements from the previous figure are compared to an element of snow exposed to morning sun and afternoon shade**.**

Notice that the PM shaded snow surface maintained temperatures similar to those of fully shaded snow, but experienced higher temperatures just before the effects of shadowing from trees took effect. Figure 6 shows surface shading on the south facing slope evident in variations in temperature. The shaded snow surface remained cooler than the snow surface in the open as a result of both shade and decreased solar zenith angle.

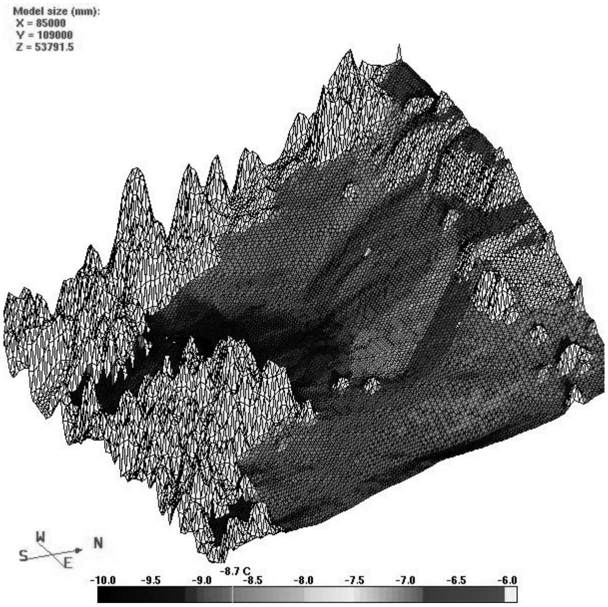

Figure 6: Snapshot of a Radtherm/RT animation of modeled surface temperatures at 0900 on March 21, 2006 for the south facing site. The darker area of snow represents cooler temperatures and is more easily seen in the color version.

The north facing slope received little direct sun, but snow in the northwest corner of the area received more solar input in the morning than other areas as is evident in Figure 7. The snow surface temperatures for a fully shaded element with a clear view of the sky and a partly shaded element with a sky view partly obstructed by trees can be seen in Figure 8. The temperatures of element A show the effects of increased solar input as well as long wave radiation exchange with adjacent trees. The effect of long wave radiation is evident in Figure 8 during the night time hours when the snow surface of element A remained warmer than element B.

Results from LIDAR models and USGS models were compared to validate future use of Radtherm/RT in areas where only USGS topographic data are available. The course grid of the model built with USGS data only allows the selection of an element containing a large area of the selected study site. As a result, elements in the USGS model are best compared to elements in the LIDAR model exposed to a clear view of the sky and free of effects from local topographic features (Figure 9). Such elements in the open areas of the LIDAR model should be affected less by local topographic features than elements adjacent to local features (e.g., trees) as seen in Figure 4; consequently, it is not surprising that the two plots in Figure 9 match very well.

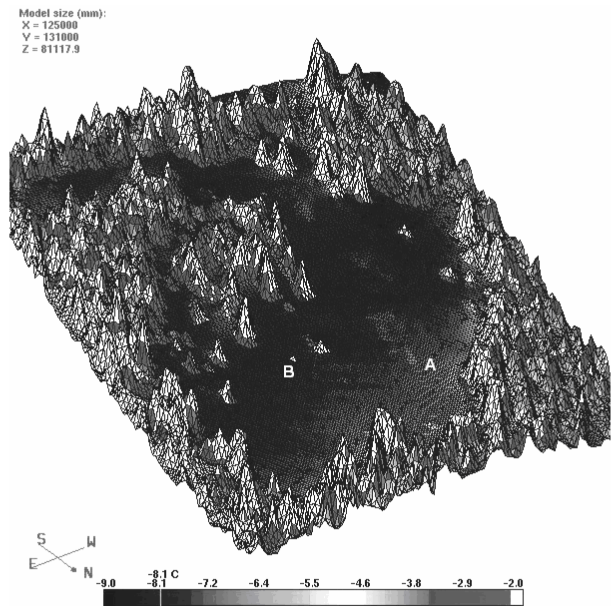

Figure 7: Snapshot of a Radtherm/RT animation of modeled surface temperatures at 1040 on March 21, 2006 for the north facing site. The lighter area of snow in the northwest corner represents warmer temperatures than other areas of snow and is more easily seen in the color version. Elements A and B are labeled in their approximate locations

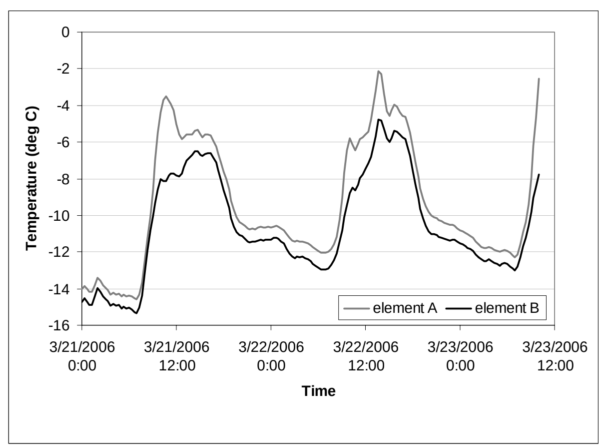

Figure 8: Modeled temperatures for two elements on the north facing site. Element A receives some direct solar radiation and does not have a clear view of the night sky because it is adjacent to the forest edge. Element B lies in a fully shaded location where it can only receive diffuse solar radiation, yet it has a relatively clear view of the night sky and remains cooler during the night time.

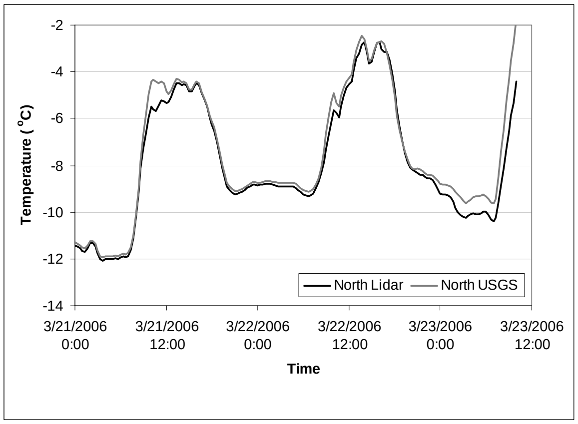

Figure 9: Comparison of modeled snow surface temperatures for carefully chosen elements on the north facing site with models built with high resolution LIDAR topographic data and much courser USGS topographic data. Similar results were obtained in the same type of comparison for the south facing site.

Measured and modeled temperatures have been compared for elements located in positions where surface temperatures were continuously measured and recorded. At this point in the model development, measured values of temperature are assumed to be correct despite possible instrumentation error. Such error is assumed to be minimal compared to the differences between modeled and measured values. Figure 10 shows a plot of measured and modeled temperature values for the south facing slope during a period between March 21 and 23, 2006.

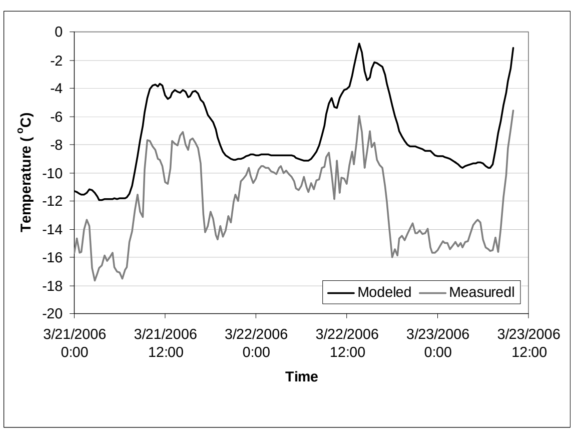

Figure 10: Comparison of modeled and measured snow surface temperatures during March 21 to 23, 2006 on the south facing slope at the location of the meteorological station.

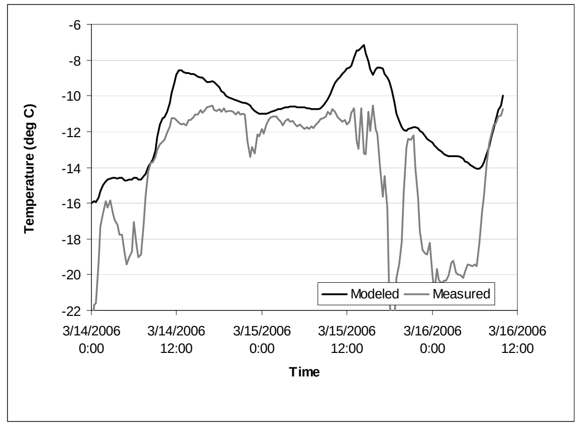

Figure 11: Comparison of modeled and measured snow surface temperatures during March 14 to 16, 2006 on the south facing slope at the location of the meteorological station.

Although modeled values of temperature result in a smoother curve, they do show the trends of measured values and major spikes in temperature. Figure 11 shows similar results for an earlier period in March. During both periods in March, measurable snow accumulated at both sites and covered upward facing instruments. On March 14, 2006 approximately 25cm of snow fell, and on March 21, 2006 approximately 5cm of snow fell. This new snow altered the surface conditions of the snowpack. As a result of this new snow, it is difficult to accurately determine the exact cause for error between the modeled and measured temperatures. However, it is speculated that snow covering the radiometers may have caused the instruments to record thermal radiation from the snow covering rather than that from the atmosphere, as a consequence yielding higher values for long wave radiation. Additionally, a better understanding of the changing thermal properties of snow is needed to produce accurate results. Relative to the snow surface temperature results, Radtherm/RT was able to more accurately predict surface temperatures of the rock outcrop located at the south facing site (Figure 12).

The measured incoming short wave and long wave radiation values used as input data for the period of March 21 to March 23 are presented in Figure 13. The diurnal fluctuations in the longwave data also indicate that the radiometer is showing a measure of thermal radiation from snow cover rather than from the sky (an error that can not readily be corrected in the current data set). Also, though the influence of incoming short wave radiation is readily apparent, the importance of long wave radiation in the energy balance should not be overlooked.

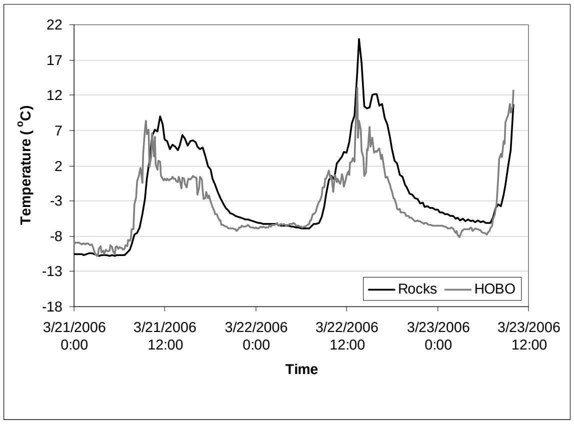

Figure 12: Comparison of modeled temperatures and temperatures measured on a rock surface with a HOBO thermistor/datalogger unit during March 21 to 23, 2006 on the rock outcrop at the south facing slope.

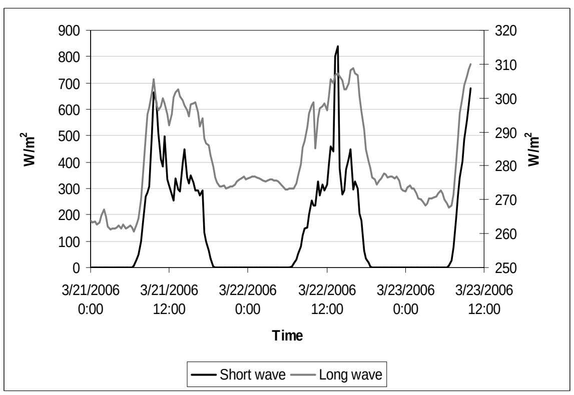

Figure 13: Measured values for incoming short (scale on left side) and long wave radiation (scale on right side) during March 21 to 23, 2006.

Mass flux was also continuously calculated for each surface element. A negative value indicates a loss of mass from the snowpack, and a positive value indicates a gain of mass. Such a gain of mass occurs in the form of condensation/deposition and is assumed to be evident as surface hoar. Quantitative measurements are difficult to obtain, and it was hoped that observations of surface hoar growth would correspond to periods of time when modeled mass flux was positive. Surface hoar crystals of 1.5 mm were observed on March 23, 2006 at 11:00AM and were assumed to have formed during the evening between March 21 and 22. However, colder snow surface temperatures were recorded the following night when the modeled temperature values were much higher (Figure 10). For this period in March, a modeled mass flux with positive values did not correlate with observations of surface hoar growth (Figure 14). Because the long wave radiation input data were assumed to be high, they were reduced by 10% to demonstrate their potential influence. This change pushed parts of the mass flux curve over zero as well as producing better results for temperature (Figure 15).

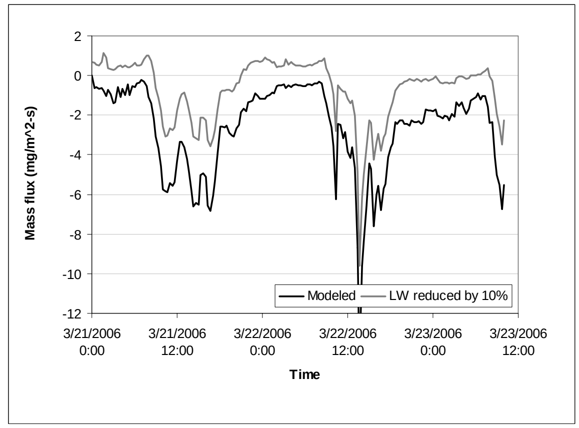

Figure 14: Modeled values for mass flux on the south facing slope. To investigate the effects of long wave (LW) radiation, the measured values of incoming LW radiation were reduced by 10%. This reduction may partially account for snow accumulation on the radiometers, and it pushes the mass flux to positive values when it is believed a layer of surface hoar formed. Similar results were obtained for mass flux on the north facing slope.

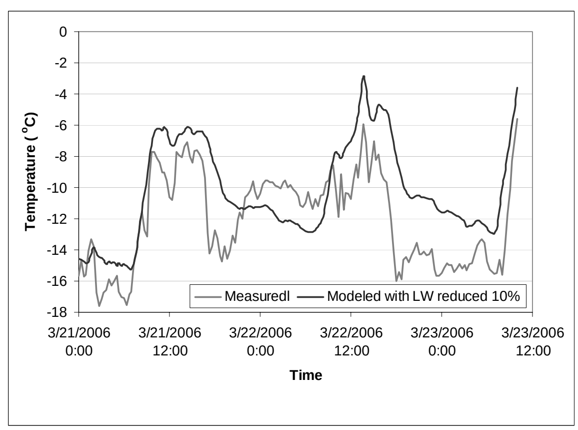

Figure 15: With the same reduction for incoming long wave radiation values as Figure 14, modeled temperature values more closely followed measured values compared to the results in Figure 10.

4. **CONCLUSIONS**

A first principles energy balance model has been used to calculate snow surface temperatures. Because these temperatures play a significant role in snow metamorphism, modeling variations in temperature in complex topography has important implications. Using Radtherm/RT, the effects of topography on the energy balance at the snow surface have been used in calculations of temperature. These effects are evident in trends in temperature and variations in temperature between selected elements. Variations in snow surface temperature for snow in the sun and shade and the temperatures for rock outcrops and trees are calculated. At this stage, these results and the trends they show should be considered a reasonable demonstration of the potential use of Radtherm/RT to account for local topography and material thermal properties.

Modeled surface temperatures for different elements have been compared to measured values. Although modeled temperatures did not match the measured temperatures, they do match the trends of measured values. Diurnal temperature swings are easily seen, and spikes in the predicted temperatures generally match spikes in the measured temperatures. At this point it appears that errors in input data and the thermal properties of snow have affected the modeled results.

Because high quality data were limited this season, the goal of this paper has been to show the utility of Radtherm/RT in modeling snow surface temperatures in complex terrain. This goal was previously accomplished by Adams et al. (2004b) for terrain on a much larger scale, and now it has been accomplished for terrain at the slope scale. Additionally, the importance of long wave radiation in the energy balance has been demonstrated and can be seen to affect both temperature and mass flux. Results from LIDAR based terrain models and USGS based terrain models were compared, and this comparison indicates the potential utility of Radtherm/RT in other areas. Upcoming seasons will see better input data and further refinement and validation of this model.

ACKNOWLEDGEMENTS

This work was possible with support from the Civil Engineering Department at Montana State University; Brian McGlynn, Department of Land Resources and Environmental Sciences at Montana State University for LIDAR data (National Science Foundation Grant BCS-0518429); the Geographic Information and Analysis Center at Montana State University for GIS help; the American Avalanche Association and 2000 International Snow Science Workshop graduate research grants for instrumentation; and Tom Leonard, Mike Cooperstein, and the Yellowstone Club Ski Patrol. The authors wish to express their sincere appreciation for such support.

REFERENCES

Adams, E.E., Gauer, P., McKittrick, L.R., and Curran, A.R., 2004a. A first principles pavement thermal model for topographically complex terrain. Transportation Research Board of the National Academies, *Transportation Research Circular*, Number E-C063, ISSN 0097-8515. 422-432.

Adams, E.E., Gauer, P., McKittrick, L.R., Curran, A.R., and Levenan, D.S., 2004b. Modeling snow temperature in complex topography. *International Symposium on Snow Monitoring and Avalanches*, Manali, H.P., India.

Adams, E.E., 1999. Proof of concept for prediction of pavement temperature: A tactical decision aid for highway safety. Final Report FHWA/MT-99-003/8117, for the State of Montana Department of Transportation.

Adams, E.E. and McDowell, S.A., 1991. Thermal model for snow on three dimensional terrain. *Proceedings of Japan-U.S. Symposium on Snow Avalanche, Landslides, Debris Flow Prediction and Control*, Tsukuba, Tsukubashi, Ibaraki-ken, Japan, Sept. 1991.

Cooperstein, M.S., Birkeland, K.W., and Hansen, K.J., 2004. The effects of slope aspect on the formation of surface hoar and diurnally recrystallized near-surface faceted crystals: Implications for avalanche forecasting. *International Snow Science Workshop. Jackson, WY*.

Etchevers, P., Martin, E., Brown, R., Fierz, C., Lejeune, Y., Bazile, E., Boone, A., Dai, Y., Essery, R., Fernández, A., Gusev, Y., Jordan, R., Koren, V., Kowalczyk, E., Nasonova, N.O., Pyles, R.D., Schlosser, A. Shmakin, A.B., Smirnova, T.G., Strasser, U., Verseghy, D., Yamazaki, T., and Yang, Z., 2004. Validation of the energy budget of an alpine snowpack simulated by several snow models (SnowMIP project). *Annals of Glaciology* 38 (1), 150-158.

Fernández, A., 1998. An Energy Balance Model of Seasonal Snow Evolution. *Physics and Chemistry of the Earth* 23 (5-6), 661-666.

Fierz, C., Riber, P., Adams, E.E., Curran, A.R., Föhn, P.M.B, Lehning, M., and Plüss, C., 2003. Evaluation of snow-surface energy balance models in alpine terrain. *Journal of Hydrology* 282, 76-94.

Hock, R., 2005. Glacier melt: a review of their processes and their modeling. *Progress in Physical Geography* 29 (3), 362-391.

Johnson, K.R., 1995. A methodology for rapid calculation of computational thermal models. SAE International Congress & Exposition, Underhood Thermal Management Session, Paper Number 951012, Detroit, MI.

Johnson, K.R., 1991. Technical Reference Guide for TCM2, Interim Report to Wright Laboratory Avionics Directorate, Wright-Patterson AFB, OH, May.

McClung, D. and P. Schaerer, 1993. *The Avalanche Handbook*. The Mountaineers, 272pp.

McKittrick, L.R., Adams, E.E., Gauer, P., Mewes, J., and Curran, A.R., 2004. Forecasting terrain dependent weather conditions: details of a model-chain sequence. Transportation Research Board of the National Academies, *Transportation Research Circular*, Number E-C063, ISSN 0097-8515. 95-108.

Prism 3.0 User's Manual, 1991, Keweenaw Research Center, Michigan Technological University, Houghton, MI, USA, 3.0 edition.